Fiber Breakage Model for Carbon Composite Stress Rupture Phenomenon: Theoretical Development and Applications

Pappu L.N. Murthy
Glenn Research Center, Cleveland, Ohio

S. Leigh Phoenix
Cornell University, Ithaca, New York

Lorie Grimes-Ledesma
Jet Propulsion Laboratory, Pasadena, California

March 2010

NASA STI Program . . . in Profile

Since its founding, NASA has been dedicated to the advancement of aeronautics and space science. The NASA Scientific and Technical Information (STI) program plays a key part in helping NASA maintain this important role.

The NASA STI Program operates under the auspices of the Agency Chief Information Officer. It collects, organizes, provides for archiving, and disseminates NASA's STI. The NASA STI program provides access to the NASA Aeronautics and Space Database and its public interface, the NASA Technical Reports Server, thus providing one of the largest collections of aeronautical and space science STI in the world. Results are published in both non-NASA channels and by NASA in the NASA STI Report Series, which includes the following report types:

- TECHNICAL PUBLICATION. Reports of completed research or a major significant phase of research that present the results of NASA programs and include extensive data or theoretical analysis. Includes compilations of significant scientific and technical data and information deemed to be of continuing reference value. NASA counterpart of peer-reviewed formal professional papers but has less stringent limitations on manuscript length and extent of graphic presentations.

- TECHNICAL MEMORANDUM. Scientific and technical findings that are preliminary or of specialized interest, e.g., quick release reports, working papers, and bibliographies that contain minimal annotation. Does not contain extensive analysis.

- CONTRACTOR REPORT. Scientific and technical findings by NASA-sponsored contractors and grantees.

- CONFERENCE PUBLICATION. Collected papers from scientific and technical conferences, symposia, seminars, or other meetings sponsored or cosponsored by NASA.

- SPECIAL PUBLICATION. Scientific, technical, or historical information from NASA programs, projects, and missions, often concerned with subjects having substantial public interest.

- TECHNICAL TRANSLATION. English-language translations of foreign scientific and technical material pertinent to NASA's mission.

Specialized services also include creating custom thesauri, building customized databases, organizing and publishing research results.

For more information about the NASA STI program, see the following:

- Access the NASA STI program home page at *http://www.sti.nasa.gov*

- E-mail your question via the Internet to *help@ sti.nasa.gov*

- Fax your question to the NASA STI Help Desk at 443–757–5803

- Telephone the NASA STI Help Desk at 443–757–5802

- Write to:
  NASA Center for AeroSpace Information (CASI)
  7115 Standard Drive
  Hanover, MD 21076–1320

Fiber Breakage Model for Carbon Composite Stress Rupture Phenomenon: Theoretical Development and Applications

Pappu L.N. Murthy
Glenn Research Center, Cleveland, Ohio

S. Leigh Phoenix
Cornell University, Ithaca, New York

Lorie Grimes-Ledesma
Jet Propulsion Laboratory, Pasadena, California

Fiber Breakage Model for Carbon Composite Stress Rupture Phenomenon: Theoretical Development and Applications

Pappu L.N. Murthy
National Aeronautics and Space Administration
Glenn Research Center
Cleveland, Ohio 44135

S. Leigh Phoenix
Cornell University
Ithaca, New York 14853

Lorie Grimes-Ledesma
National Aeronautics and Space Administration
Jet Propulsion Laboratory
Pasadena, California 91109

Abstract

Stress rupture failure of Carbon Composite Overwrapped Pressure Vessels (COPVs) is of serious concern to Science Mission and Constellation programs since there are a number of COPVs on board space vehicles with stored gasses under high pressure for long durations of time. It has become customary to establish the reliability of these vessels using the so called classic models. The classical models are based on Weibull statistics fitted to observed stress rupture data. These stochastic models cannot account for any additional damage due to the complex pressure-time histories characteristic of COPVs being supplied for NASA missions. In particular, it is suspected that the effects of proof test could significantly reduce the stress rupture lifetime of COPVs. The focus of this paper is to present an analytical appraisal of a model that incorporates damage due to proof test. The model examined in the current paper is based on physical mechanisms such as micromechanics based load sharing concepts coupled with creep rupture and Weibull statistics. For example, the classic model cannot accommodate for damage due to proof testing which every flight vessel undergoes. The paper compares current model to the classic model with a number of examples. In addition, several applications of the model to current ISS and Constellation program issues are also examined.

Nomenclature

α	Weibull shape parameter for composite strength
β	Weibull exponent and shape parameter for composite lifetime under fixed fiber stress
θ	creep exponent for matrix
ρ	power law breakdown exponent reflecting sensitivity of lifetime to fiber stress
σ	fiber stress
σ_p	fiber stress at proof pressure level
σ_{ref}	characteristic fiber stress level
$\hat{\sigma}_V$	composite reference strength (same as σ_{ref})
ζ	Weibull shape parameter for fiber strength
$F(t)$	cumulative distribution function for composite failure

k'	same as $\hat{k}$
$\hat{k}$	critical fiber break cluster size for catastrophic failure
k_p	fiber break cluster size after proof
$R(t)$	vessel reliability over time
t	time in hours
t_c	characteristic time for creep to occur
t_c	characteristic time for matrix creep
t_p	hold time at proof pressure
$t_{p,b}$	proof benefit time scale
t_{ref}	characteristic time scale for fiber failure

Introduction

Carbon composite overwrapped pressure vessels (COPVs) are widely used for storing gasses under high pressure in a wide range of applications including onboard spacecraft such as the Space Shuttle and the International Space Station (ISS). The use of COPVs is currently being planned for the Crew Exploration and launch vehicles as well. The principal advantage of the carbon COPV technology over conventional all metallic storage devices is the substantial weight savings. The National Aeronautics and Space Administration (NASA) has been supporting the development of this technology since the early 1970s (Ref. 1) with an interest in safe application of these components to reduce mass to orbit. NASA Johnson Space Flight Center White Sands Test Facility (WSTF) in collaboration with NASA Jet Propulsion Laboratory (JPL) has been testing components in support of this objective since the 1980s and WSTF has been involved in test development and analysis to address effects of impact, propellant and cryogenic fluids exposure on Kevlar (DuPont)/epoxy and carbon/epoxy composite overwrapped pressure vessels (Ref. 2).

Space flight COPVs are generally made of a thin metallic liner overwrapped with a high strength fiber/epoxy composite. This design allows for significant weight savings in contrast to an all metal pressure vessel design and these vessels are widely used for spacecraft and commercial applications because of this advantage. Mechanisms associated with the failure of the COPV system must be considered for safe operation from manufacturing to disposal. The fibrous composite overwrap carries a significant portion of the pressure load during operation and therefore is subjected to a possible stress rupture failure mode. Stress rupture is manifested as sudden, catastrophic failure of the overwrap, and is a function of fiber stress ratio in the composite and time at pressure.

Stress Rupture Phenomenon

As mentioned before, failure due to stress rupture is one of the major concerns with the usage of COPVs. A thorough discussion of various approaches to compute reliability under stress rupture failure is given in the NASA Engineering Safety Center (NESC) Carbon ITA report (Ref. 3). In recent publications, both Thomas and Robinson (Refs. 4 and 5) have provided models for determinations of reliability which included their interpretation of model parameters based on carbon/epoxy stress rupture data available at the time of their publications. The industry practice is to utilize these early models. The Thomas model was chosen to develop the stress rupture requirements in the COPV industry standard, AIAA SO–81–2000 (Ref. 6).

Thomas and Robinson models used in the COPV industry are based on Weibull distributions for lifetime, yet they are fundamentally different in structure. Both were generated to allow the fitting of stress rupture data without physics based interpretation to other composite behavior, such as strength, and neither is based on the fundamental fiber behavior such as single fiber failure mechanisms. The Robinson model is based on a Weibull power law and the Thomas model is derived from a Weibull exponential framework. These two frameworks were originally suggested by Reference 7. In addition, the work of Phoenix (Ref. 8) suggests the power law framework has more flexibility and is self-consistent with other, but related, composite properties such as strength. A history of these models with detailed comparison of the exponential and power law forms is given in the volume II of the NESC Carbon Report in Appendix L (Ref. 8). Due to the limitations in the Thomas and Robinson models, the Phoenix power law framework model was used in the NESC COPV Independent Investigation. The results from this model are consistent with the Robinson model as well. The remainder of the current paper focuses on the Phoenix classic model, and its limitations due to lack of physics and the subsequent improvements proposed by Phoenix which is named the fiber breakage model. A thorough discussion of these models is given in the Appendix L of the NESC Carbon Report Volume II.

In the current paper the classic model of Phoenix is reviewed and its limitations are illustrated when proof testing of COPVs is included in the model. This is followed by a theoretical development and applications of a more sophisticated fiber breakage model that incorporates the proof test induced damage for the reliability computations of carbon COPVs. Proof testing COPVs after fabrication is conceptually viewed as a process of weeding out weak vessels. Vessels are most often removed because of liner leakage, but rarely from catastrophic failure of the composite overwrap. Nevertheless, unlike the situation with metal vessels, considerable damage is done by a proof test in terms of breaking carbon fibers and possibly strands. Classical reliability models are typically not based on fiber breakage processes in a way that captures the above drawbacks of proof testing. In fact, when applied to carbon/epoxy COPVs, the power law-Weibull version of the classical model predicts that the higher the proof test level, the greater the benefit in terms of improved reliability. The fiber breakage model explicitly accounts for the micromechanics based statistical failure processes in composites consisting of carbon fibers in epoxy matrix.

Classic Model: A Review

The usual reliability model for failure of a composite is a parametric model in a Weibull power-law framework that embodies a memory integral for past fiber history, $\sigma(s)$, $0 < s \le t$. The distribution function for overall composite failure is given by

$$F\left(t;\sigma(\circ)\right)=1-\exp\left\{-\left[\frac{1}{t_{\text{ref}}}\int_0^t\left(\frac{\sigma(s)}{\sigma_{\text{ref}}}\right)^\rho ds\right]^\beta\right\}, \quad t>0 \tag{1}$$

where ρ is the power law breakdown exponent reflecting sensitivity of lifetime to fiber stress level, β is a Weibull exponent that happens to be the Weibull shape parameter for composite lifetime under fixed fiber stress, and σ_{ref} and t_{ref} are characteristic stress and time scale constants for the composite material. Thus a stress history for a pressure vessel in stress rupture may be idealized as

$$\sigma_p(s)=\begin{cases}\sigma_p, & 0<s<t_p \\ \sigma, & t_p<t\end{cases} \tag{2}$$

where σ_p is the proof level and t_p is the proof hold time, typically a few minutes, and t is overall time that may stretch to thousands of hours. Then the distribution function for lifetime (including failure times during proof) is

$$F\left(t;\sigma_p\left(\circ\right)\right)=1-\exp\left\{-\left[\left(\frac{\sigma_p}{\sigma_{\text{ref}}}\right)^\rho\frac{t_p}{t_{\text{ref}}}+\left(\frac{\sigma}{\sigma_{\text{ref}}}\right)^\rho\frac{t-t_p}{t_{\text{ref}}}\right]^\beta\right\}\tag{3}$$

The conditional distribution for lifetime given *survival* of the proof test is

$$F\left(t\,|\,\sigma,\sigma_p\right)=1-\frac{1-F\left(t;\sigma_p\left(\circ\right)\right)}{1-F\left(t_p;\sigma_p\left(\circ\right)\right)}$$

$$=1-\exp\left\{-\left[\left(\frac{\sigma_p}{\sigma_{\text{ref}}}\right)^\rho\frac{t_p}{t_{\text{ref}}}\right]^\beta\left(\left[1+\left(\frac{\sigma}{\sigma_p}\right)^\rho\frac{t-t_p}{t_p}\right]^\beta-1\right)\right\}\tag{4}$$

For times much longer than the proof time (a few minutes) and well within a proof benefit timescale, $t_{p,b}$, whereby $t-t_p\approx t$ applies, this can be rewritten as

$$F\left(t\,|\,\sigma,\sigma_p\right)\approx1-\exp\left\{-\left[\left(\frac{\sigma_p}{\sigma_{\text{ref}}}\right)^\rho\frac{t_p}{t_{\text{ref}}}\right]^\beta\beta\left(\frac{\sigma}{\sigma_p}\right)^\rho\frac{t}{t_p}\right\},\quad 0<t_p\ll t\ll t_{p,b}\tag{5}$$

where

$$\beta\left(\frac{\sigma}{\sigma_p}\right)^\rho\frac{t_{p,b}}{t_p}=1\quad\text{or}\quad t_{p,b}\approx\frac{t_p}{\beta}\left(\frac{\sigma_p}{\sigma}\right)^\rho\tag{6}$$

is the timescale over which the formula applies and a proof benefit exists, since the quantity after the square parentheses is of order unity or smaller (typically $\beta\ll1$ for carbon fiber composites). For very long times $t_{p,b}\ll t$ the probability of failure follows

$$F\left(t\,|\,\sigma,\sigma_p\right)\approx1-\exp\left\{-\left[\left(\frac{\sigma}{\sigma_{\text{ref}}}\right)^\rho\frac{t}{t_{\text{ref}}}\right]^\beta\left(\left[1+\left(\frac{\sigma_p}{\sigma}\right)^\rho\frac{t_p}{t}\right]^\beta-\left[\left(\frac{\sigma_p}{\sigma}\right)^\rho\frac{t_p}{t}\right]^\beta\right)\right\}$$

$$\approx1-\exp\left\{-\left[\left(\frac{\sigma}{\sigma_{\text{ref}}}\right)^\rho\frac{t}{t_{\text{ref}}}\right]^\beta\left(1+\beta\left(\frac{\sigma_p}{\sigma}\right)^\rho\frac{t_p}{t}-\left[\left(\frac{\sigma_p}{\sigma}\right)^\rho\frac{t_p}{t}\right]^\beta\right)\right\}\tag{7}$$

and the proof benefit fades.

These results can be written in terms of the conditional reliability given by $R\left(t\,|\,\sigma,\sigma_p\right)=1-F\left(t\,|\,\sigma,\sigma_p\right)$. For times within the proof benefit range up to time $t_{p,b}$ we have

$$R\left(t\,|\,\sigma,\sigma_p\right) \approx \exp\left\{-\left[\left(\frac{\sigma_p}{\sigma_{\text{ref}}}\right)^\rho\frac{t_p}{t_{\text{ref}}}\right]^\beta \beta\left(\frac{\sigma}{\sigma_p}\right)^\rho\frac{t}{t_p}\right\}, \quad 0 < t_p \ll t \ll t_{p,b} \tag{8}$$

and for times $t_{p,b} \ll t$ we have

$$R\left(t\,|\,\sigma,\sigma_p\right) \approx \exp\left\{-\left[\left(\frac{\sigma}{\sigma_{\text{ref}}}\right)^\rho\frac{t}{t_{\text{ref}}}\right]^\beta\left(1+\beta\left(\frac{\sigma_p}{\sigma}\right)^\rho\frac{t_p}{t}-\left[\left(\frac{\sigma_p}{\sigma}\right)^\rho\frac{t_p}{t}\right]^\beta\right)\right\} \tag{9}$$

Thus, according to the classic model, the reliability benefit of the proof test and how long it lasts are strongly related to the values of β and ρ, and these vary widely among fiber types. For instance, for Kevlar/epoxy composites, typically $1 < \beta < 2$ and $\rho < 30$ but for carbon/epoxy composites typically $\beta < 0.3$ and $\rho > 70$.

Finally we also consider a proof test followed by a long survival time, t_s, and calculate the conditional reliability for future lifetime of the same order of magnitude as that already survived. The probability of failure by time $t > t_s$ (including failures during proof and up to time t_s)

$$F\left(t;\sigma_p(\circ)\right) = 1-\exp\left\{-\left[\left(\frac{\sigma_p}{\sigma_{\text{ref}}}\right)^\rho\frac{t_p}{t_{\text{ref}}}+\left(\frac{\sigma}{\sigma_{\text{ref}}}\right)^\rho\frac{t_s-t_p}{t_{\text{ref}}}+\left(\frac{\sigma}{\sigma_{\text{ref}}}\right)^\rho\frac{t-t_s}{t_{\text{ref}}}\right]^\beta\right\} \tag{10}$$

Noting that $t_p \ll t_s < t$ and using the above methods, the conditional reliability given survival to time t_s is found to be approximately

$$R\left(t\,|\,\sigma,\sigma_p,t_s\right) \approx \exp\left\{-\left[\left(\frac{\sigma_p}{\sigma_{\text{ref}}}\right)^\rho\frac{t_p}{t_{\text{ref}}}\right]^\beta\left[\left(1+\left(\frac{\sigma}{\sigma_p}\right)^\rho\frac{t}{t_p}\right)^\beta-\left(1+\left(\frac{\sigma}{\sigma_p}\right)^\rho\frac{t_s}{t_p}\right)^\beta\right]\right\} \tag{11}$$

These results will be compared to those from the stochastic fiber breakage model derived below.

Deficiencies of Classic Model

To illustrate the effects of proof test on reliability, the relevant equations mentioned above are shown plotted for both Kevlar and carbon in Figure 1. For Kevlar fibers the parameters chosen are $\rho = 24$, $\beta = 1.625$ and $t_{\text{ref}} = 1.43$. These are typical values for Kevlar and are currently used in reliability calculations of the Orbiter COPVs. A comprehensive database of stress rupture life data for Carbon fibers, however, is not available. Limited data for strands and vessels are available in literature. In the current computations the chosen parameters are $\rho = 72$, $\beta = 0.35$ and $t_{ref} = 0.001$. These are the parameter values for a typical Carbon COPV based on the limited available data. Proof test is assumed for 5 min at a fiber stress ratio of 0.667 and the operating stress ratio is assumed to be 0.5. The dashed lines show the base line case of no proof test. The dot-dashed lines show the case of effect of proof test on reliability for both Kevlar and carbon composites stress rupture performance. The solid lines show the conditional reliability where credit is taken for surviving the proof test. For Kevlar composites the proof test appears to have a minimal impact on the overall reliability for a period of about one year beyond which all three
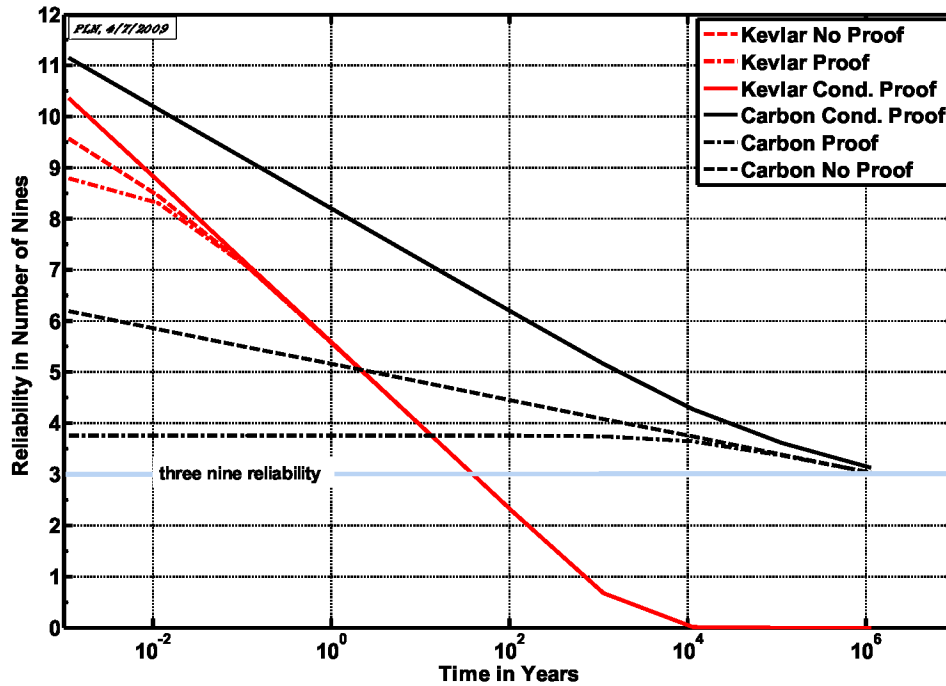
Figure 1.—Effect of proof test on reliability of Kevlar and carbon COPVs.

cases are virtually indistinguishable. However, for carbon proof test appears to have substantial impact on the reliability for extremely long periods of time. The effects for this particular case appear to last in excess of 100,000 yr. Furthermore, the conditional reliability where credit is taken for surviving the proof test itself appears to increase by several orders of magnitude compared to the straight calculated reliability. Also, the proof test itself (dot-dashed line) appears to cost a significant amount of reliability in number of nines although it is only for a short duration. In general if one were to put a three-nine reliability as a minimum requirement, then carbon COPVs appear to last several times longer under stress than Kevlar COPVs. It is for this reason, carbon overwrapped pressure vessels are becoming more popular alternatives to the Kevlar counter parts in space applications.

In conclusion, if the classic model is correct, the proof test benefit for Kevlar fiber is relatively short lived while that for the carbon fiber could last for any conceivable lifetime of the vessel, provided that $\rho > 70$. However, the model is based on purely curve fitting to statistical stress rupture data. Any damage that may have resulted during proof test is not accounted for in the model. Furthermore the model in its current form indicates that higher the proof stress ratio, the better it is for reliability provided the vessels survive proof test. As the proof test stress ratio increases composites tend to accumulate damage in terms of fiber breakage which will have adverse effects to its performance. By considering the process of fiber failure more explicitly, we investigate whether the classic model is a realistic reflection of the failure process in the case of carbon/epoxy composites or whether it is a misleading idealization.

Fiber Breakage Model Development

The fiber breakage model theoretical development is discussed in detail in References 8 and 9. For sake of completeness, this discussion is included in Appendix A. Key equations that are needed for discussion here are shown below while the details are deferred to the Appendix A. The life time

distribution function (probability of failure for $T \leq t$ for composite under stress σ which has gone through a proof test at σ_p a hold period of t_p is given by Equation (A.31) in Appendix A:

$$H_V\left(t;\sigma,\sigma_p\right) \approx 1 - \exp\left\{\left(\sigma_p/\hat{\sigma}_V\right)^{\hat{\alpha}}\left(\sqrt{1+\left(t_p/t_c\right)^{\theta}}\right)^{\hat{k}-1}\right.$$
$$\left. \times\left[1+\left(\sigma/\sigma_p\right)^{\varsigma}\left(\sqrt{\left(1+\left(t/t_c\right)^{\theta}\right)\Big/\left(1+\left(t_p/t_c\right)^{\theta}\right)}-1\right)\right]^{\hat{k}-k_p}\right\}, \quad t > t_p \tag{12}$$

where $\hat{\sigma}_V$ composite reference strength (same as σ_{ref}), $\hat{k}$ is critical fiber break cluster size for catastrophic failure, k_p is fiber break cluster size after proof, ς is Weibull shape parameter for fiber strength, and θ is the matrix creep exponent. $\hat{\alpha}$ is given by the product $\hat{k}\varsigma$. The fiber break cluster size after proof k_p is given by Equations (A.29.a) and (A.29.b) in Appendix A.

$$k_p = \left\lfloor \frac{4}{\pi}\left[\left(\frac{\sigma_p}{\sigma}\right)^2 - 1\right] + 1\right\rfloor$$

or $\tag{13}$

$$k_p \approx \frac{4}{\pi}\left[\left(\frac{\sigma_p}{\sigma}\right)^2 - 1\right] + 1$$

The conditional reliability given that any weak vessels removed by proof test is given by the following equation (App. A, Eq. (A.35))

$$R\left(t\mid\sigma,\sigma_p\right) \approx \exp\left\{-\left(\sigma_p/\hat{\sigma}_V\right)^{\hat{\alpha}}\left(\sqrt{1+\left(t_p/t_c\right)^{\theta}}\right)^{\hat{k}-1}\right.$$
$$\left. \times\left(\left[1+\left(\sigma/\sigma_p\right)^{\varsigma}\left(\sqrt{\left(1+\left(t/t_c\right)^{\theta}\right)\Big/\left(1+\left(t_p/t_c\right)^{\theta}\right)}-1\right)\right]^{\hat{k}-k_p}-1\right)\right\}, \quad 0 < t_p < t \tag{14}$$

Finally for the case where the vessel has not undergone any proof test the reliability is given by

$$R(t\mid\sigma) \approx \exp\left\{-\left(\sigma/\hat{\sigma}_V\right)^{\hat{\alpha}}\left(\sqrt{1+\left(t/t_c\right)^{\theta}}\right)^{\hat{k}-1}\right\}, \quad 0 < t \tag{15}$$

Equations (5) to (7) can now be used to perform comparison studies to classic model for COPVs.

Comparison of Classic Model Versus the Fiber Breakage Model

To compare the predictions of classic model to fiber breakage model, a T1000G COPV with a nominal stress ratio of 50 percent is considered. The proof factor (defined as the ratio of fiber stress at proof to fiber stress at operating conditions) is 1.5 which gives a stress ratio of 0.667. These are typical values for such vessels. The model parameters for T1000G fiber are taken as:

Classic model:

$$\rho = 114; t_{c,\text{ref}} = 0.001\,\text{hr}; \beta = 0.22; \tag{16}$$

Fiber breakage model:

$$\zeta = 5; t_c = 0.01\,\text{hr}; \hat{k} = 5; t_p = 0.0833\ \text{hr}; \hat{\alpha} = \hat{k}\zeta \tag{17}$$

Predictions of reliability of T1000G COPV expressed as "number of nines" are shown plotted as a function of time for both the models in Figure 2. Calculations are shown for both no proof test case and the case where survival of a proof test conducted at 66.7 percent stress ratio for 5 min.

Both models predict almost identical reliability when proof is not considered, but the classic model predicts vastly improved reliability when conditional survival of proof test is taken into account. However, the fiber breakage model predicts much lower reliabilities when proof test effects are included and the reliabilities are based upon conditional survival of proof test. A loss of two nines in reliability is possible due to proof test as indicated in Figure 2. The reason for this divergent behavior is due to the fact that the fiber breakage model takes into account fiber damage that takes place during the proof test. It is for this reason recommended that the level of proof test be carefully determined such that excessive damage to fibers is avoided.

Parameter Sensitivities and Uncertainties

The sensitivity of reliability to changes in various parameters is shown in Figure 3. Here each parameter is varied with respect to its nominal value. The nominal values chosen for the parameters are for the T1000G carbon fiber and are given by Eq. (10).

$$\zeta = 5; t_c = 0.01\,\text{hr}; \hat{k} = 5; t_p = 0.0833\,\text{hr}; \hat{\alpha} = \hat{k}\zeta\ ;$$
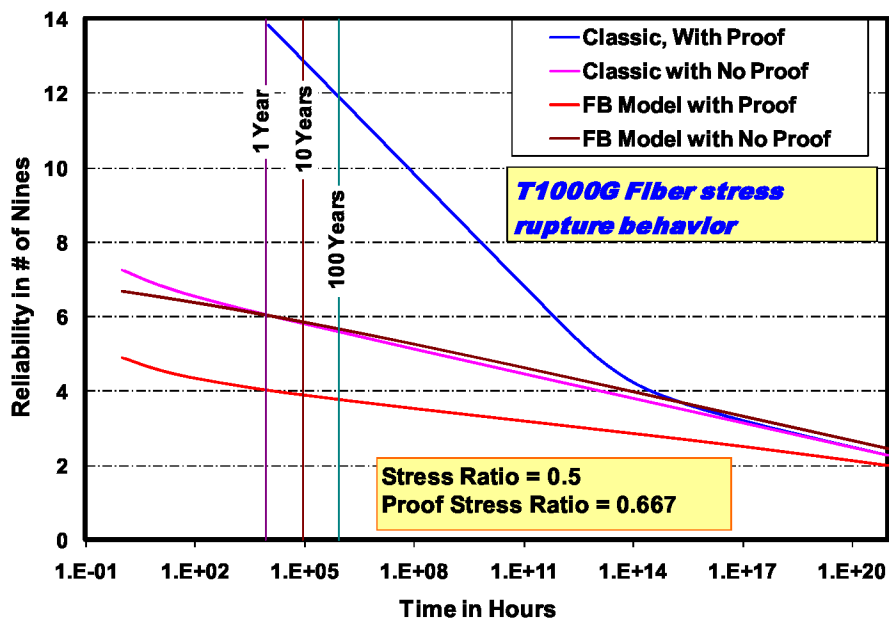
Figure 2.—Comparison of classic and fiber breakage model reliability predictions for a T1000G COPV operating at a stress ratio of 50 percent.

Stress ratio considered is 50 percent and proof stress ratio is 75 percent. Each parameter is made dimensionless by dividing with nominal values and the dimensionless parameters are varied from 0.7 to 1.3, one at a time. The reliability of the vessels conditional on proof test survival is computed for 10,000 hr and is shown plotted versus all the parameters.

It is clear from the figure that the Reliability shows a high degree of sensitivity to changes in the parameters ζ followed by k' and θ. The parameters t_c and t_p have very little or no effect on the reliability. Determination of the three most important parameters to a high degree of accuracy is therefore essential to assess the reliability of the vessel accurately.

In general when dealing with reliability one must assess and account for two types of uncertainties: epistemic uncertainty and aleatory uncertainty. Epistemic uncertainty arises due to lack of knowledge, or insufficient data. Such uncertainties can be reduced over time with more experiments and experience. On the other hand aleatory uncertainty is the so called physical variability that is present in almost all the systems and is unlikely to be reducible. Various publications address these two types of uncertainty and the importance of separating and resolving them (Refs. 9 and 10).

These uncertainties are especially critical for the COPVs because of the risks and costs involved. Parameter or epistemic uncertainty can be reduced by collecting more data and by developing better analytical models. Here we attempt to show how the model form uncertainties affect the reliability estimates via Monte Carlo simulations of the conditional probability of survival. As an example a typical vessel made of T1000G is chosen which has been successfully on flight for the past 7 yr. The parameters that are considered uncertain with the respective distribution statistics are given Table I. These values are taken from the References 3 and 11. An observation of interest is the fact that the variability in parameters is rather high. This is due to very limited stress rupture data that is available for this class of materials (Ref. 11). The variability in parameters is established based on this limited data and one can expect to reduce this when more data is available thus improving the reliability considerably.

The proof stress ratio is taken to be 0.75 and proof test time $t_p = 5$ min. The stress ratio for the vessel is taken as 0.478. These values are typical of the highest loaded COPV on the ISS. Reliability conditional upon surviving successfully the past history of 7 yr is computed using both classic model and the fiber breakage model and are reported in Table II. The calculations are repeated for missions up to the year 2016, 2020 and 2030 starting from year 2009 which represents a past history of 7 yr. In these calculations it has been assumed that the vessel is at the maximum expected operating pressure (MEOP).
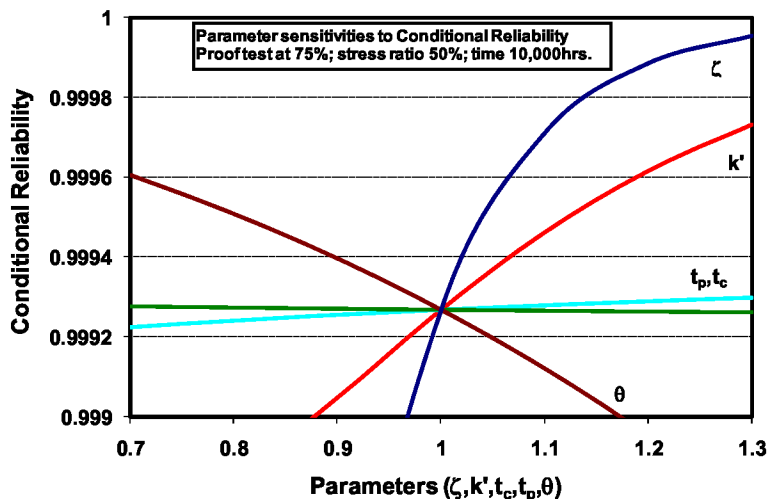

Figure 3.—Reliability of a T1000G Carbon fiber COPVs for 10,000 hr as a function of various model parameters.

However, typical COPVs experience a ramp reduction in pressure with time as the gas is used. The assumption that the COPVs maintain MEOP is conservative for operation beyond the conditional point and unconservative for the past history. However, in this example case, the assumption of MEOP operation before the conditional point did not contribute significantly to the reliability and was neglected.

TABLE I.—PARAMETERS USED FOR CLASSIC AND FIBER BREAKAGE
MODELS IN THE UNCERTAINTY SIMULATION STUDIES

Classic Model Parameters			
Parameter	Mean	COV	Distribution
ρ	114	0.25	Lognormal
β	0.22	0.3	Lognormal
t_{ref}	0.001	1.0	Lognormal
Fiber Breakage Model Parameters			
Parameter	Mean	COV	Distribution
ς	5	0.25	Lognormal
θ	0.11	0.25	Lognormal
k'	5	0.3	Lognormal
t_c	0.01	1.0	Lognormal

TABLE II.—RELIABILITY PREDICTIONS FOR A TYPICAL CARBON COPV ON SERVICE
CONDITIONAL ON SURVIVAL OF 7 YR OF PAST HISTORY AT MEOP TO OUT YEARS

2500 psi operating (Stress ratio = 0.478)	2016 (70,080 hr)	2020 (105,120 hr)	2030 (192,720 hr)
Point	0.999943	0.999925	0.99988
Mean	0.999521	0.999279	0.99894
95%	0.99768	0.99738	0.99615

Three different estimates point, mean and the 95 percent confidence are computed by running thousands of Monte Carlo simulations Reliabilities are conditional on successful past history of 7 yr. As seen in the table, the classic model does predict a slightly higher reliability (three effects. The classic model predictions are based on neglecting the proof test effects because if proof test were included, the reliability would be very high as suggested in Figure 2. The 95 percent confidence estimates, however, fall slightly short off the three nine mark in this example. As can be expected the reliabilities can be increased by reducing the pressure if the three nine reliability to the end of the mission is absolutely critical to the program.

The second example in this section pertains to hypothetical reliability assessment of next generation launch vehicle. Here the various models and predictions are assessed and compared for a system of COPVs made of T1000G fiber. Because the vessels have not been manufactured, the exact stress ratio is not known. For purposes of this initial analysis, a proof factor of 1.25 and a design burst factor (DBF) of 2.0 are assumed. The stress ratio is given approximately by. In Figure 4, the DBF is varied from 1.5 to 3.0 and proof factor is scaled appropriately from the 2.0 DBF case. Reliability is computed for both classic and fiber breakage models. Tables III and IV show the details of the classic and fiber breakage model parameter values chosen in the reliability computations.

TABLE III.—CLASSIC MODEL CASE 1 AND 2 PARAMETER VALUES

Classic Model 1	
Parameter	Nominal value
ρ	114
β	0.22
t_{ref}	0.001
Classic Model 2	
Parameter	Nominal value
ρ	72
β	0.35
t_{ref}	0.001

TABLE IV.—FIBER BREAKAGE MODEL PARAMETER VALUES

Fiber Breakage Model Parameters (High variability)			
ς	5	0.25	Lognormal
θ	0.11	0.25	Lognormal
k'	5	0.25	Lognormal
t_c	0.01	0.3	Lognormal
Fiber Breakage Model Parameters (Low variability)			
ς	5	0.05	Lognormal
θ	0.11	0.05	Lognormal
k'	5	0.05	Lognormal
t_c	0.01	0.05	Lognormal

The simulation results based on the above four models are shown in Figure 4. The two classic models are chosen to represent the case of no prior proof test and the case where proof stress induced damage is accounted. Thus the classic model case 2 parameters are chosen to simulate reduced performance due to possible proof test fiber damage. Two fiber breakage models one with a high degree of variability and one with low variability are considered to represent the current state of knowledge and a future state of knowledge with better understanding of carbon stress rupture behavior and the availability of a comprehensive stress rupture database. Thus, the high variability of fiber breakage model represents the current status of the limited data and knowledge of carbon stress rupture behavior. The low variability case represents what we can expect for reliability in future when our knowledge base of stress rupture behavior for T1000G fiber is enhanced through substantial stress rupture testing and establishing a comprehensive data base. As can be seen from the figure, for a COPV system of 13 vessels, and a DBF of 2, the reliability can vary from a little over one nine to five nines depending upon the model chosen. The uncertainty in reliability high lights the overwhelming need for a formal development of an experimental stress rupture testing program
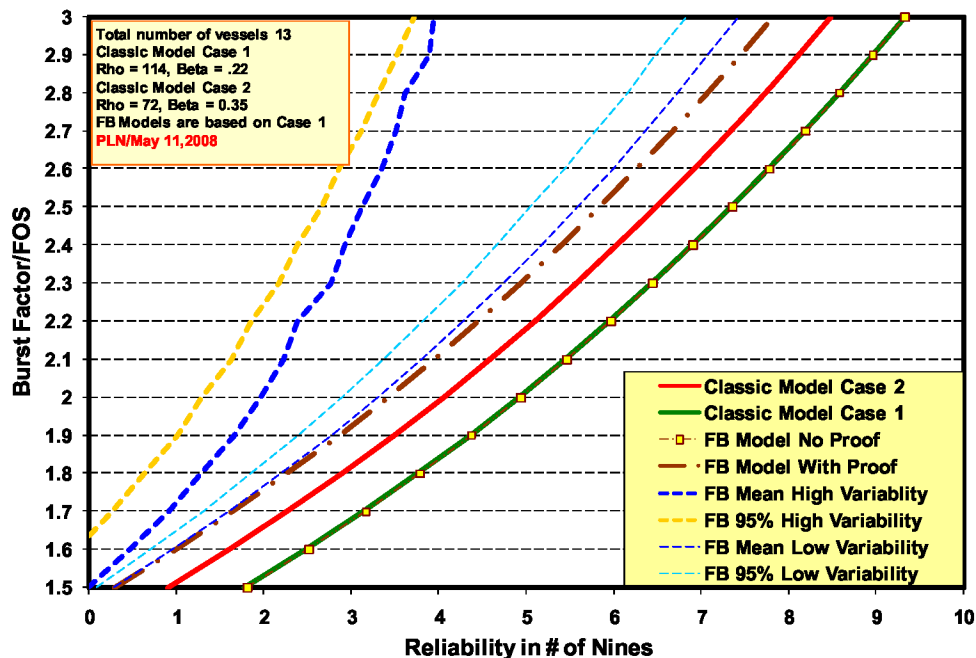

Figure 4.—Various model predictions of reliability of a system of vessels on board a launch vehicles for a total mission time of 1 yr.

Summary

Stress rupture life and reliability of COPVs for space applications are assessed by using two different models with some illustrative examples. The classic model while simple to use has the short comings of not able to represent directly the proof test induced fiber damage. The conditional reliability based upon survival of proof test shows unrealistically high value when classic model is used. The reliability appears to increase as the proof stress ratio increases and its effect lasts for thousands of years. This is clearly an artifact of the model which is purely phenomenological model and lacks physics. Proof tests performed at higher loads induce fiber damage due to scatter in fiber strength and that is not captured in this phenomenological model. In order to address this micromechanics based fiber breakage model is proposed. The model accounts for possible fiber damage due to proof test. However, this model gives overly conservative reliability estimates. Some of this conservatism is due to lack of sufficient data for the T1000G carbon fiber that is considered in the simulations. This introduces huge uncertainty in the parameter estimates which translate into substantial reductions in reliability estimates.

The wide range of reliability estimates depending upon which model is used warrants immediate attention to the development of a formal experimental test plan to reduce this uncertainty and narrow down the differences between the models or formulate better analytical models based on the comprehensive test data. Furthermore, the fiber breakage model is based on progressive damage theory which has not been rigorously tested and validated. Currently the NESC is planning to address some of these issues by a detailed stress rupture testing that include proofed strands and vessels as well as un-proofed test articles. It is anticipated that the tests will provide more clarity to various models and help reduce the uncertainties as well as improve some of the models. The results will be reported in subsequent papers.

References

1. Lark, R.F., 1977, "Recent Advances in Lightweight, Filament-Wound Composite Pressure Vessel Technology," NASA TM–73699
2. 2 Beeson, H.; D. Davis; W.R. Ross, Sr.; and R. Tapphorn, January 2002. Composite Overwrapped Pressure Vessels, NASA Technical Paper NASA/TP—2002-210769, Johnson Space Center, Houston TX.
3. "Shelf Life Phenomenon and Stress Rupture Life of Carbon/Epoxy Composite Overwrapped Pressure Vessels (COPVs)," Technical Consultation Report, Vol. I and II, NASA NESC Report RP–06–83, Sep. 14, 2006.
4. Thomas, D.A. "Long-life assessment of graphite/epoxy materials for Space Station Freedom pressure vessels," J. of Propulsion, Vol. 8, 1992, pp. 87–92.
5. Robinson, E.Y. "Design Prediction for Long-Term Stress Rupture Service of Composite Pressure Vessels," The Aerospace Corporation Report Number ATR-62(2743)-1, 1991.AIAA SO-81-2000
6. ANSI/AIAA S-081-2000, Space Systems-Composite Overwrapped Pressure Vessels (COPVs), 2000
7. Coleman, B.D., "Statistics and Time Dependence of mechanical breakdown in fibers," J. of Applied Physics, 29, 1958, pp. 968–983
8. "Shelf Life Phenomenon and Stress Rupture Life of Carbon/Epoxy Composite Overwrapped Pressure Vessels (COPVs)," Technical Consultation Report, Vol. II, NASA NESC Report RP-06-83, Sep. 14, 2006.
9. Helton J.C. and D.E. Burmaster. "Treatment of Aleatory and Epistemic Uncertainty in Performance Assessments for Complex Systems," Reliability Engineering and System Safety: Special Issue on Aleatory and Epistemic Uncertainties, 54, 1996, p. 91.
10. Hoffman F.O. and J.S. Hammonds, J.S., "Propagation of Uncertainty in Risk Assessments: The Need to Distinguish Between Uncertainty Due to Lack of Knowledge and Uncertainty Due to Variability," Reliability Engineering and System Safety, 14 (1994): 707.
11. DeTeresa, S.J., and S.E. Groves. "Properties of fiber composites for advanced flywheel energy storage devices," Lawrence Livermore National Laboratory Report UCRL–JC–142020, Jan.12, 2001.

Appendix A
Stochastic Fiber Breakage Model Development
Micromechanics and Statistics of Fiber Failure Process

To gain a deeper understanding of the issue we first discuss the failure process in the composite in terms of fiber stress redistribution around fiber breaks (i.e., load sharing) and local break cluster formation among a large number of fiber elements of length, δ_e, which is the characteristic elastic load transfer length from a broken fiber to an intact neighbor. This length will be compared later to a length $\delta(t)$ that grows with time beyond a characteristic time scale t_c for matrix creep in shear around initial and evolving fiber breaks in a cluster. Note that t_c is of the same order of magnitude as the "proof hold time", t_n, in a proof test. Also δ_e depends on many mechanical and geometric quantities, the most important being the fiber diameter, d_f, the fiber Young's modulus, E_f, the matrix shear modulus, G_m, and the effective width of matrix between the fibers, w_m, which depends on the fiber volume fraction, V_f. For fully elastic behavior $\delta_e \approx 2d_f\sqrt{E_f w_m/(G_m d_f)}$ and since $140 \leq E_f/G_m \leq 200$, $w_m/d_f \approx 0.3$, and $d_f \approx 5$ μm we obtain $\delta_e \approx 20d_f \approx 0.1$ mm.

There are a large number of such fiber elements in the overwrap of a typical carbon/epoxy pressure vessel. A single yarn or tow typically has 12,000 fibers, and one wrap covers about 2.5 mm of width around the vessel circumference and is 0.25 mm thick. For a COPV of diameter 75 cm, the overwrap thickness may be 4 mm corresponding to 8 overwrap layers. Thus for a typical carbon/epoxy pressure vessel there are of the order of 10^{12} fiber elements of length δ_e in the overwrap. Later in the analysis, the volume, V, of the overwrap will be the number of such fiber elements of length δ_e that it contains.

The probability that a fiber element of length δ_e breaks under stress σ is well approximated by a Weibull distribution of the form

$$F_{\delta_e}(\sigma) = 1 - \exp\left\{-(\delta_e/l_0)(\sigma/\sigma_{l_0})^\zeta\right\},$$
$$= 1 - \exp\left\{-(\sigma/\sigma_{\delta_e})^\zeta\right\}, \qquad \sigma > 0$$

(A.1)

where l_0 is a typical tension test gage length for fiber testing (e.g., 1 cm) with associated Weibull scale parameter σ_{l_0}, and shape parameter ζ estimated from such testing. Also σ_{δ_e} is the Weibull scale parameter for the strength of a fiber element of length, δ_e. Implicit in the above formula is the scaling of fiber strength with length following

$$\sigma_{\delta_e} = \sigma_{l_0}(\delta_e/l_0)^{-1/\zeta}$$

(A.2)

which reflects the fact that that carbon fibers typically follow Weibull weakest-link statistics. Typically $\zeta \approx 5$ for carbon fibers so the length effect is fairly strong. A ten-fold decrease in length increases the strength by about 58 percent. A useful approximation for $F_{\delta_e}(\sigma)$, especially in the lower tail, is

$$F_{\delta_e}(\sigma) \approx (\sigma/\sigma_{\delta_e})^\rho, \quad 0 < \sigma < \sigma_{\delta_e}$$

(A.3)

The characteristic strength, σ_{δ_e}, is typically about 3 times the effective stress level, σ_V, or $\sigma_{\delta_e} \approx 3\sigma_V$.

Next we consider the fiber stress level $\sigma \ll \sigma_{\delta_e}$ and proceed towards calculating the probability of formation of a cluster of size k emanating from a given fiber element of length δ_e in the composite. Note

that the number of such "initial" breaks is a random variable that is binomially distributed with parameters V and $F_{\delta_e}(\sigma)$. The mean number of such breaks is $n(\sigma) \approx VF_{\delta_e}(\sigma)$, and thus, does not depend on the calculated value of δ_e since $\sigma << \sigma_{\delta_e}$ so that breaks are far apart. In fact only a small proportion of the fiber elements fail under the applied stress, σ. For instance, for $\sigma/\sigma_V = 0.50$, or a fiber stress ratio of 50 percent, we have $\sigma_{\delta_e} \approx 3\sigma_V \approx 6\sigma$ and for $\zeta \approx 5$ the probability of failure of a given fiber element is approximately $(\sigma/\sigma_{\delta_e})^p \approx (1/6)^5 \approx 1.3 \times 10^{-4}$. Thus, about one in every 8,000 fiber elements fails under stress σ and along a fiber the breaks are about 78 cm apart. While this may seem to be a large spacing, the number of such broken fiber elements in the overwrap is roughly $n(\sigma) \approx VF_{\delta_e}(\sigma)$ $\approx (1.3 \times 10^{-4})(10^{12}) = 1.3 \times 10^8$, still a very large number.

All of this assumes a homogeneous or uniform stress field. If there are areas of stress concentration, say near a boss where failure is more likely to occur, then a relatively smaller volume of material might be at a higher stress concentration, and thus, the breaks may be more concentrated. There still will be a large number of fiber elements in this region of higher stress and the breaks will be more frequent, i.e., more closely spaced. By themselves these initial breaks obviously do not cause composite failure and some micromechanical interaction is necessary to generate break clusters that eventually become unstable. This is pursued next.

Derivation of Composite Strength Distribution

The failure process can be characterized in simplified terms as follows: First is the growth of clusters of fiber breaks. In order to fail the composite one of these clusters must grow to a critical size. Locally the formation of a cluster begins with failure of a single fiber element of length δ_e under stress σ followed by failure of a neighboring element under the stress concentration $K_1\sigma$, and another neighbor under higher stress concentration $K_2\sigma$ (since there are now two adjacent breaks) and so on until the size reaches k. (The stress concentration factors grow unbounded and satisfy $1 < K_1 < K_2 < \dots$.) The probability of formation of such a cluster is approximately

$$W_k(\sigma) \approx c_k F_{\delta_e}(\sigma) F_{\delta_e}(K_1\sigma) F_{\delta_e}(K_2\sigma) \cdots F_{\delta_e}(K_{k-1}\sigma)$$
$$\approx c_k (K_1 K_2 \cdots K_{k-1})^\zeta (\sigma/\sigma_{\delta_e})^{k\zeta}$$

(A.4)

where c_k is a combinatorial factor capturing all the possible configurations (in terms of sequence of fiber breaks) that a cluster can have. For instance, in a planar array of fibers with load shedding primarily to nearest surviving fibers (one on each side) it can be shown that

$$K_j \approx \sqrt{1 + \pi j/4}, \quad j = 0,1,2,\cdots$$

(A.5)

and

$$c_k \approx 2^{k-1}$$

(A.6)

The factor $c_k = 2^{k-1}$ captures the fact that, except for the failure of the given fiber element to start the cluster, there are typically two overloaded neighbors next to the growing cluster at any growth step. At applied fiber stress level, σ, the critical value of k that triggers a catastrophic cascade is called k_σ and satisfies

$$K_{k_\sigma-1}\sigma < \sigma_{\delta_e} < K_{k_\sigma}\sigma$$

(A.7)

since beyond this value of k_σ all neighboring fiber elements to the cluster will be overloaded well beyond their characteristic strengths σ_{δ_e}. Once this occurs, their individual probabilities of failure now exceed 0.632 and with further cluster growth rapidly approach unity so that the cascade cannot be stopped.

In a hexagonal or 'random' array of fibers the ideas are similar but c_k will grow much more rapidly than in above planar case and will involve products of increasing numbers of fibers around the periphery of a growing approximately circular cluster. However the values of $K_1, K_2, \cdots, K_k, \cdots$ will grow more slowly. For instance, it can be shown that

$$K_j \approx \sqrt{1 + D/\pi}, \quad D \approx \sqrt{4j/\pi}, \quad j = 0, 1, 2, \cdots \tag{A.8}$$

and

$$c_k \approx \pi^{k-1} \prod_{j=1}^{k-1} \left(\sqrt{4j/\pi} + 1 \right) \tag{A.9}$$

where D is approximately the cluster diameter, and $j = \pi D^2/4$ is approximately the number of fiber breaks in the cluster.

It can be shown that the distribution function for the strength of the composite at a fiber stress level σ is approximately

$$H_V(\sigma) \approx 1 - \exp\left[-V W_{\hat{k}}(\sigma) \right] \tag{A.10}$$

which can be written as the Weibull distribution

$$H_V(\sigma) \approx 1 - \exp\left[-(\sigma/\hat{\sigma}_V)^{\hat{\alpha}} \right] \tag{A.11}$$

where

$$\hat{\sigma}_V = \sigma_\delta \left(V c_{\hat{k}} \right)^{-1/(\hat{k}\zeta)} \left(K_1 K_2 \cdots K_{\hat{k}-1} \right)^{-1/\hat{k}} \tag{A.12}$$

and

$$\hat{\alpha} = \hat{k}\zeta \tag{A.13}$$

and where

$$K_{\hat{k}-1} \hat{\sigma}_V < \sigma_{\delta_e} < K_{\hat{k}} \hat{\sigma}_V \tag{A.14}$$

which is equivalent to $\hat{k} = k_{\hat{\sigma}_V}$.

In the above description we ignore the fact that k_σ increases slowly as σ decreases (whereby the probability of composite failure typically decreases by more than an order of magnitude with each integer valued increase in k_σ). Instead we have chosen the particular value, $\hat{k}$, called the critical cluster size for catastrophic fracture, when the stress level is equal to the Weibull scale parameter for composite strength. In this case $\hat{k}$ satisfies

$$K_{\hat{k}} \hat{\sigma}_V \approx \sigma_{\delta_e} \tag{A.15}$$

This equation implies that the predicted strength distribution for the composite is not actually a straight line but is slightly curved on a Weibull plot and becomes steeper at lower stresses implying slightly lower probabilities of failure than a straight Weibull line would predict. Typically the change in slope is so small that it cannot be detected in pressure vessel testing and carbon/epoxy strand testing with typical number of test samples. However it has been very clearly detected in the experimental testing of seven fiber micro-composites on a repeatable basis (Refs. A.1 and A.2) and is seen also in Monte Carlo simulations (Ref. A.3). Furthermore there is some evidence that as structures become larger their variability in strength decreases, which is consistent with the increasing steepness feature above.

Composite Lifetime Distribution in Stress Rupture in Absence of Initial Proof Test

Stress rupture in carbon fiber composites arises mainly because the matrix creeps in shear around fiber breaks. A useful model is that this creep follows a power law creep compliance of the form

$$J_m(t) = J_{m,e}\left[1 + (t/t_c)^\theta\right], \quad t \geq 0 \tag{A.16}$$

where $J_{m,e}$ is the instantaneous elastic creep compliance ($J_{m,e} = 1/G_{m,e}$), where $G_{m,e}$ is the instantaneous elastic shear modulus), t_c is the characteristic time for creep to occur (at which time the compliance $J_m(t)$ has effectively doubled), and θ is the creep exponent. The creep exponent is a crucial parameter and depends on such factors as the matrix and interface chemistry in terms of adhesion to the fiber, fiber volume fraction, and temperature—to name the most important influences. Typically $0.1 < \theta < 0.5$ for epoxies, and note that as a reference point the value $\theta = 1$ corresponds to a Newtonian viscous material. We note that nonlinear forms of the creep function described in terms of visco-plasticity introduce a dependence on shear stress level between the fibers raised to some power larger than unity (i.e., 3 or 4). However this modifies the analysis in only modest ways and does not influence the conclusions.

It can be shown that, under the power-law creep compliance, the characteristic load transfer length around a fiber break is time dependent following

$$\delta(t) = \delta_e\sqrt{1 + (t/t_c)^\theta}, \quad t \gg 0$$
$$\approx \delta_e(t/t_c)^{\theta/2}, \quad t \gg t_c \tag{A.17}$$

where δ_e is again the instantaneous elastic load transfer length. Thus as t increases, this overload length grows so that increasing numbers of flaws in fibers adjacent to a break cluster of size k are exposed to stress $K_k\sigma$ and can fail despite surviving the original stress level σ.

Susceptibility to such delayed failure is greatly enhanced for carbon fibers with high variability in strength, i.e., low values for the Weibull shape parameter, ζ, for strength. Individual carbon fibers are virtually immune to stress rupture compared to that seen in carbon/epoxy composites. Essentially single fibers under constant stress fail on loading or do not fail at all. Of course, in the composite matrix creep makes it possible for the stresses on fibers next to broken fibers to increase and so the main cause of their failure is increasing stress around growing clusters.

In stress rupture at a fixed stress level, $\sigma < \hat{\sigma}_V$, *and assuming* no *previous stress excursion above this level (such as a proof test)*, the lifetime distribution function can be derived as a modification of the case above. The distribution function for composite lifetime follows

$$H_V(t;\sigma) \approx 1 - \exp\left[-VW_{\hat{k}}(t;\sigma)\right], \quad t \gg t_c \tag{A.18}$$

where $W_{\hat{k}}(t;\sigma)$ is a characteristic distribution function given in simplified form by

$$W_{\hat{k}}(t;\sigma) \approx c_{\hat{k}}\left(K_1 K_2 \cdots K_{\hat{k}-1}\right)^{\zeta}\left(\sigma/\sigma_{\delta_e}\right)^{\hat{k}\zeta}\left(\sqrt{1+\left(t/t_c\right)^{\theta}}\right)^{\hat{k}-1}$$

$$\approx c_{\hat{k}}\left(K_1 K_2 \cdots K_{\hat{k}-1}\right)^{\zeta}\left(\sigma/\sigma_{\delta_e}\right)^{\hat{k}\zeta}\left(t/t_c\right)^{(\hat{k}-1)\theta/2}, \quad t \gg t_c \tag{A.19}$$

This form reflects the fact that at a given element location the creep-rupture process requires failure of that element simply due to the applied stress, followed by the failure of some element out of $2\sqrt{1+\left(t/t_c\right)^{\theta}}$ neighboring fiber elements along the adjacent fibers exposed to the overload $K_1\sigma$, where the number exposed grows over time as the load transfer lengths grows. This process continues as more and more elements fail in time and ultimately these time dependent failures in a cluster number $\hat{k}-1$. Fiber breaks occur sequentially so there is some time lag for growth of the new overload length at each new fiber failure site, but this is not reflected in the above formula where time is just the original time, t. Simulations show, however, that the effect is small compared to the long timescales involved (Ref. A.3). A more refined analysis would lead to the need for the multiplicative factor of the form,

$$\Theta(\hat{k}) = \Gamma(\theta/2+1)\Big/\Gamma\left[(\hat{k}-1)\theta/2+1\right] \tag{A.20}$$

where $\Gamma(z)$ is the usual gamma function. However, typically $0.05 < \theta < 0.25$, and unless $\hat{k}$ is extremely large, this factor is not significantly different from unity and can be neglected.

The resulting Weibull approximation is

$$H_V(t;\sigma) \approx 1 - \exp\left[-\left(t/\hat{t}_V(\sigma)\right)^{\hat{\beta}}\right], \quad t \gg t_c \tag{A.21}$$

where

$$\hat{\beta} = (\hat{k}-1)\theta/2 \tag{A.22}$$

and

$$\hat{t}_V = t_c\left(\sigma/\hat{\sigma}_V\right)^{-\hat{\rho}} \tag{A.23}$$

are the respective Weibull shape and scale parameters for lifetime. Also

$$\hat{\rho} = \left[\hat{k}\big/(\hat{k}-1)\right]\rho \tag{A.24}$$

and

$$\rho = 2\zeta/\theta \tag{A.25}$$

are the power-law exponents for lifetime versus stress level, being the effective value and large cluster limit, respectively.

In summary, in a stress rupture setting the applied stress, σ, is much smaller than the scale parameter for tensile strength, $\hat{\sigma}_V$, so that the probability of failure on initial loading, $H_V(\sigma)$, is easily satisfies the

reliability requirement. However, probabilities of failure at much larger times $t \gg t_c$ become the key concern. Essentially, the first failure at some location (necessary to start the matrix creep process) is due to a flaw in the fiber element of elastic length $\delta = \delta_e$, and the remaining failures occur due to the time dependent matrix creep process since the overload lengths quickly grow beyond δ_e for $t \gg t_c$. Since we assume no initial overload (such as a proof test), the initial clusters of breaks due to the initial loading are automatically consumed by those that occur in time since any fiber that fails initially is automatically included in time dependent failures. Another important fact inherited from linear viscoelasticity is that $\hat{k}$ for stress rupture is almost the same as $\hat{k}$ for strength at times near zero, so we do not distinguish between the two.

Effect of Proof Testing

As mentioned, proof tests are often applied to pressure vessels to some fiber stress level, σ_p, in order to filter out weak vessels. For all metal pressure vessels this process can be argued to be all beneficial with no drawbacks, i.e., no new damage is introduced; however the situation is far less clear in composite over-wrapped pressure vessels. The difference is that, because of the proof test, many fiber elements will now fail under the higher stress σ_p, that would not have failed under the lower stress-rupture stress level, σ. These additional failures now provide many additional locations for subsequent cluster growth in stress-rupture.

For instance, the number $n(\sigma_p)$ of fiber breaks at the proof stress level σ_p divided by the number $n(\sigma)$ at the stress-rupture level σ is given by

$$n\left(\sigma_p\right)\big/n(\sigma) = \left(\sigma_p\big/\hat{\sigma}_V\right)^{\zeta}\big/\left(\sigma\big/\hat{\sigma}_V\right)^{\zeta} = \left(\sigma_p\big/\sigma\right)^{\zeta} \tag{A.26}$$

For the typical value $\zeta = 5$ and $\sigma_p/\sigma = 1.5$ we obtain $n(1.5\sigma)/n(\sigma) = (1.5)^5 = 7.6$. Thus, there are 7.6 times as many single fiber breaks or 'singlets' due to the proof test as without the proof test and these additional singlets now become many more seeds for stress-rupture compared to those that would occur without the proof test. The situation is made worse, however, since some singlets among the expanded group (from the proof test) will generate many failing neighbors due to the overload $K_1\sigma_p$ that would not occur due to the milder overload $K_1\sigma$, thus forming additional 'doublets' of failed fibers. Furthermore some of the neighbors to these new doublets will fail under $K_2\sigma_p$ but not under $K_2\sigma$, thus forming additional 'triplets', and so on. In essence, as a result of the proof test, there will be a distribution of fiber break multiplets of various sizes, and the numbers of such multiplets of each size will be much larger than would have occurred without the proof test.

A proof test to stress level, σ_p, will eliminate any vessel that develops a cluster that reaches critical size, which for simplicity we take to be $\hat{k}$, i.e., a weak vessel. Unfortunately it suddenly creates many clusters that would not occur otherwise. This is very different from the model for metals or ceramics, where the proof test may eliminate any vessels with flaws or cracks larger than critical, but anything smaller will actually be beneficially blunted and no new ones will be created. In ceramics the model is similar, though each smaller crack may grow slightly. It must be noted, however, that the fiber itself benefits from the proof test in that the vast majority of the fiber elements that survive the proof stress level, σ_p, cannot fail until the stress level in the future exceeds σ_p due to some overload $K_j\sigma$ next to a sufficiently large cluster.

Next we consider an initial proof test to fiber stress level, σ_p, over time $0 < t < t_p$ (typically involving a 'proof hold time' of a few minutes) and let $W_{\hat{k}}\left(t;\sigma,\sigma_p\right)$ be the characteristic distribution function for

lifetime extending the concepts developed earlier, except we now have two stress levels, σ and σ_p. We then have

$$H_V(t;\sigma) \approx 1 - \exp\left\{ -VW_{\hat{k}}(t;\sigma_p,\sigma_p) \right\}, \qquad 0 < t < t_p \tag{A.27}$$

the time period up to t_p, where

$$W_{\hat{k},p}(t;\sigma,\sigma_p) \approx c_{\hat{k}}(K_1 K_2 \cdots K_{\hat{k}-1})^\zeta (\sigma_p/\sigma_{\delta_e})^{\hat{k}\zeta} \left(\sqrt{1+(t/t_c)^\theta} \right)^{\hat{k}-1}, \quad 0 < t < t_p \tag{A.28}$$

This is identical to the form earlier except that now $\sigma = \sigma_p$.

We now consider the effect of the stress decreasing from σ_p to σ for $t > t_p$. Although further growth of the overload length on fibers next to a break cluster continues at approximately the same rate, the overstress itself is now reduced by the factor σ/σ_p. Thus the rate at which new breakable flaws are encountered is reduced nominally through the Weibull factor $(\sigma/\sigma_p)^\zeta$. The overall effect is nominally equivalent to the stress remaining at level σ_p, but the rate of increase of the overload length being slowed in time by the factor $(\sigma/\sigma_p)^\zeta$. This characterization, however, is not entirely correct since all fiber elements have been proof tested to σ_p and any further fiber element failure requires a growing overload length around some cluster of size j, such that $K_j\sigma > \sigma_p$. The critical size for such a cluster is denoted $k_p = k_p(\sigma/\sigma_p)$ and satisfies

$$K_{k_p-1}\sigma < \sigma_p < K_{k_p}\sigma \quad \text{or} \quad K_{k_p-1} < \sigma_p/\sigma < K_{k_p} \tag{A.29.a}$$

Thus any cluster of size k_p after the proof test will continue to grow, and smaller ones will not. We see that $\sigma_p/\sigma > 1$ requires $k_p \geq 1$ and using $K_k \approx \sqrt{1+\pi k/4}$, $k = 1,2,3...$ we can see that

$$k_p = \left\lfloor \frac{4}{\pi}\left[\left(\frac{\sigma_p}{\sigma}\right)^2 - 1 \right] + 1 \right\rfloor \tag{A.29.b}$$

where $[z]$ refers to the integer part of z. In computations, it suffices simply to use

$$k_p \approx \frac{4}{\pi}\left[\left(\frac{\sigma_p}{\sigma}\right)^2 - 1 \right] + 1 \tag{A.29.c}$$

Thus for $t_p < t$ we obtain

$$W_{\hat{k},p}(t;\sigma,\sigma_p) \approx c_{\hat{k}}(K_1 K_2 \cdots K_{\hat{k}-1})^\zeta (\sigma_p/\sigma_{\delta_e})^{\hat{k}\zeta} \left(\sqrt{1+(t_p/t_c)^\theta} \right)^{k_p-1}$$

$$\times \left[\sqrt{1+(t_p/t_c)^\theta} + (\sigma/\sigma_p)^\zeta \left(\sqrt{1+(t/t_c)^\theta} - \sqrt{1+(t_p/t_c)^\theta} \right) \right]^{\hat{k}-k_p} \tag{A.30}$$

Using again (A.23) for $\hat{\sigma}_V$, we reduce (A.41) to

$$VW_{\hat{k},p}\left(t;\sigma,\sigma_p\right) \approx \left(\sigma_p/\hat{\sigma}_V\right)^{\hat{\alpha}} \left(\sqrt{1+\left(t_p/t_c\right)^{\theta}}\right)^{\hat{k}-1}$$

$$\times \left\{1+\left(\sigma/\sigma_p\right)^{\varsigma}\left(\sqrt{1+\left(t/t_c\right)^{\theta}}\Big/\sqrt{1+\left(t_p/t_c\right)^{\theta}}-1\right)\right\}^{\hat{k}-k_p} , \quad t>t_p \tag{A.31}$$

and finally

$$H_V\left(t;\sigma,\sigma_p\right) \approx 1-\exp\left\{\left(\sigma_p/\hat{\sigma}_V\right)^{\hat{\alpha}}\left(\sqrt{1+\left(t_p/t_c\right)^{\theta}}\right)^{\hat{k}-1}\right.$$

$$\left.\times \left[1+\left(\sigma/\sigma_p\right)^{\varsigma}\left(\sqrt{\left(1+\left(t/t_c\right)^{\theta}\right)\Big/\left(1+\left(t_p/t_c\right)^{\theta}\right)}-1\right)\right]^{\hat{k}-k_p}\right\}, \quad t>t_p \tag{A.32}$$

Conditional Reliability After a Proof Test

Next we must evaluate the conditional reliability given that any weak vessels removed by the proof test. The conditional reliability given survival, is

$$R\left(t\mid\sigma,\sigma_p\right) = \exp\left\{-V\left[W_{\hat{k},p}\left(t;\sigma,\sigma_p\right)-W_{\hat{k},p}\left(t_p;\sigma_p,\sigma_p\right)\right]\right\} \tag{A.33}$$

where the characteristic distribution function in time, t, beyond the proof time is

$$VW_{\hat{k},p}\left(t;\sigma,\sigma_p\right) \approx \left(\sigma_p/\hat{\sigma}_V\right)^{\hat{\alpha}} \left(\sqrt{1+\left(t_p/t_c\right)^{\theta}}\right)^{\hat{k}-1}$$

$$\times \left\{1+\left(\sigma/\sigma_p\right)^{\varsigma}\left(\sqrt{1+\left(t/t_c\right)^{\theta}}\Big/\sqrt{1+\left(t_p/t_c\right)^{\theta}}-1\right)\right\}^{\hat{k}-k_p} , \quad t_p<t \tag{A.34.a}$$

whereas

$$VW_{\hat{k},p}\left(t;\sigma,\sigma_p\right) \approx \left(\sigma_p/\hat{\sigma}_V\right)^{\hat{\alpha}} \left(\sqrt{1+\left(t_p/t_c\right)^{\theta}}\right)^{\hat{k}-1} \quad 0<t\le t_p \tag{A.34.b}$$

Thus the conditional reliability, (A.44), becomes

$$R\left(t\mid\sigma,\sigma_p\right) \approx \exp\left\{-\left(\sigma_p/\hat{\sigma}_V\right)^{\hat{\alpha}}\left(\sqrt{1+\left(t_p/t_c\right)^{\theta}}\right)^{\hat{k}-1}\right.$$

$$\left.\times\left(\left[1+\left(\sigma/\sigma_p\right)^{\varsigma}\left(\sqrt{\left(1+\left(t/t_c\right)^{\theta}\right)\Big/\left(1+\left(t_p/t_c\right)^{\theta}\right)}-1\right)\right]^{\hat{k}-k_p}-1\right)\right\}, \quad 0<t_p<t \tag{A.35}$$

Two particular cases are of interest: If the proof time t_p is such that $\left(t_p/t_c\right)^{\theta} \ll 1$, then we approximately have

$$R\left(t\mid\sigma,\sigma_p\right)\approx\exp\left\{-\left(\frac{\sigma_p}{\hat{\sigma}_V}\right)^{\hat{\alpha}}\left(\left[1+\left(\sigma/\sigma_p\right)^{\zeta}\left(\sqrt{1+\left(t/t_c\right)^{\theta}}-1\right)\right]^{\hat{k}-k_p}-1\right)\right\},\quad 0<t_p<t \qquad (A.36)$$

On the other hand if $\left(t_p/t_c\right)^{\theta}\approx 1$, then approximately

$$R\left(t\mid\sigma,\sigma_p\right)\approx\exp\left\{-\left(\frac{\sigma_p}{\hat{\sigma}_V}\right)^{\hat{\alpha}}2^{(\hat{k}-1)/2}\left(\left[1+\left(\frac{\sigma}{\sigma_p}\right)^{\zeta}\left(\frac{1}{\sqrt{2}}\sqrt{1+\left(\frac{t}{t_c}\right)^{\theta}}-1\right)\right]^{\hat{k}-k_p}-1\right)\right\},\quad t_c<t \qquad (A.37)$$

We can see that the behavior of the reliability in (A.48) depends on the magnitude of the time t relative to a transition time $\hat{t}_{p,b}$ that solves

$$\left(\frac{\sigma}{\sigma_p}\right)^{\zeta}\left(\frac{1}{\sqrt{2}}\sqrt{1+\left(\frac{\hat{t}_{p,b}}{t_c}\right)^{\theta}}-1\right)=1 \qquad (A.38)$$

or

$$\hat{t}_{p,b}=t_c\left\{2\left(\sigma_p/\sigma\right)^{2\zeta}+2\sqrt{2}\left(\sigma_p/\sigma\right)^{\zeta}\right\}^{1/\theta} \qquad (A.39)$$

Then for moderate times such that $t_c<<t<<\hat{t}_{p,b}$ we can expand the (A.48) to obtain

$$R\left(t\mid\sigma,\sigma_p\right)\approx\exp\left\{-2^{\hat{k}/2-1}\left(\hat{k}-k_p\right)\left(\frac{\sigma_p}{\hat{\sigma}_V}\right)^{\hat{\alpha}}\left[\left(\frac{\sigma}{\sigma_p}\right)^{\rho}\left(\frac{t}{t_c}\right)\right]^{\theta/2}\right\},\quad t_c<<t<<\hat{t}_{p,b} \qquad (A.40)$$

where again $\rho=2\zeta/\theta$. On the other hand for extremely long times beyond the threshold time $\hat{t}_{p,b}$, we obtain from (A.48) a different expansion of the form

$$R\left(t\mid\sigma,\sigma_p\right)=\exp\left\{-2^{\hat{k}/2-1}\left(\frac{\sigma_p}{\hat{\sigma}_V}\right)^{\hat{\alpha}}\left[\left(\frac{\sigma}{\sigma_p}\right)^{\rho}\left(\frac{t}{t_c}\right)\right]^{\hat{\beta}_p}\right\},\quad \hat{t}_{p,b}<<t \qquad (A.41)$$

where

$$\hat{\beta}_p=\left(\hat{k}-k_p\right)\theta/2 \qquad (A.42)$$

Proof Test and Survival to Some Long Time

Finally we consider the conditional reliability for the case where the there was originally a proof test but the pressure vessel has also survived for a long time $t_s>>t_c$. Then the reliability can be shown to be

$$R_V\left(t\,|\,\sigma,\sigma_p,t_p,t_s\right) \approx \exp\left\{-\left(\frac{\sigma_p}{\hat\sigma_V}\right)^{\hat\alpha}\left[\sqrt{1+\left(\frac{t_p}{t_c}\right)^\theta}\,\right]^{\hat k-1}\left(\left[1+\left(\frac{\sigma}{\sigma_p}\right)^\zeta\left(\sqrt{\left[1+\left(\frac{t}{t_c}\right)^\theta\right]\Big/\left(1+\left(\frac{t_p}{t_c}\right)^\theta\right)}-1\right)\right]^{\hat k-k_p}\right.\right.$$

$$\left.\left.-\left[1+\left(\frac{\sigma}{\sigma_p}\right)^\zeta\left(\sqrt{\left[1+\left(\frac{t_s}{t_c}\right)^\theta\right]\Big/\left(1+\left(\frac{t_p}{t_c}\right)^\theta\right)}-1\right)\right]^{\hat k-k_p}\right)\right\},\quad t_s<t$$

(A.43)

For $\left(t_p/t_c\right)^\theta\approx1$ we can simplify the above to

$$R_V\left(t\,|\,\sigma,\sigma_p,t_p,t_s\right) \approx \exp\left\{-\left(\frac{\sigma_p}{\hat\sigma_V}\right)^{\hat\alpha}2^{(\hat k-1)/2}\left(\left[1+\left(\frac{\sigma}{\sigma_p}\right)^\zeta 2^{-1/2}\left(\sqrt{1+\left(\frac{t}{t_c}\right)^\theta}-1\right)\right]^{\hat k-k_p}\right.\right.$$

$$\left.\left.-\left[1+\left(\frac{\sigma}{\sigma_p}\right)^\zeta 2^{-1/2}\left(\sqrt{1+\left(\frac{t_s}{t_c}\right)^\theta}-1\right)\right]^{\hat k-k_p}\right)\right\},\quad t_s<t$$

(A.44)

Also for intermediate times satisfying $t_c\ll t\ll\hat t_{p,b}$ this expands to

$$R\left(t\,|\,\sigma,\sigma_p\right)\approx\exp\left\{-2^{\hat k/2-1}\left(\hat k-k_p\right)\left(\frac{\sigma_p}{\hat\sigma_V}\right)^{\hat\alpha}\left[\left(\frac{\sigma}{\sigma_p}\right)^\rho\left(\frac{t_s}{t_c}\right)^{\theta/2}\right]\left(\left(\frac{t}{t_s}\right)^{\theta/2}-1\right)\right\},\quad t_c\ll t\ll\hat t_{p,b}\qquad(A.45)$$

However, for extremely long times $\hat t_{p,b}\ll t$ we have

$$R\left(t\,|\,\sigma,\sigma_p\right)=\exp\left\{-2^{\hat k/2-1}\left(\frac{\sigma_p}{\hat\sigma_V}\right)^{\hat\alpha}\left[\left(\frac{\sigma}{\sigma_p}\right)^\rho\left(\frac{t_s}{t_c}\right)^{\hat\beta_p}\right]\left(\left(\frac{t}{t_s}\right)^{\hat\beta_p}-1\right)\right\},\quad\hat t_{p,b}\ll t\qquad(A.46)$$

where

$$\hat\beta_p=\left(\hat k-k_p\right)\theta/2\qquad(A.47)$$

Comparison of Stochastic Fiber Breakage Model and Classic Model in Case of a Proof Test

We can compare the results of the classic model and the stochastic fiber breakage model to see what the key differences are. For the classic model we assume $t_p\approx t_{\rm ref}\ll t_c$ and naturally let $\sigma_{\rm ref}=\hat\sigma_V$ and $\alpha=\beta\rho$. Then

$$R\left(t\,|\,\sigma,\sigma_p\right)\approx\exp\left\{-\beta\left(\frac{\sigma_p}{\hat\sigma_V}\right)^{\alpha}\left(\frac{\sigma}{\sigma_p}\right)^{\rho}\frac{t}{t_p}\right\},\quad 0<t_p\ll t\ll t_{p,b}\qquad(A.48)$$

where

$$t_{p,b}\approx\frac{t_p}{\beta}\left(\frac{\sigma_p}{\sigma}\right)^{\rho}\qquad(A.49)$$

Note that the expression (A.59) for the conditional reliability contains the fundamental factor

$$\Phi_p=\beta\left(\frac{\sigma}{\sigma_p}\right)^{\rho}\frac{t}{t_p}\qquad(A.50)$$

In the classical model Φ_p is linear in time, t, so early on when, $0<t_p\ll t\ll t_{p,b}$, we find that Φ_p is very small and captures the reliability improvement due to the proof test.

In the stochastic fiber breakage model just developed and with a short proof test hold, $0<t_p\ll t_c$ the situation is different in that we have

$$R\left(t\,|\,\sigma,\sigma_p\right)\approx\exp\left\{-\left(\hat k-k_p\right)\left(\frac{\sigma_p}{\hat\sigma_V}\right)^{\hat\alpha}\left[\left(\frac{\sigma}{\sigma_p}\right)^{\rho}\left(\frac{t}{t_c}\right)\right]^{\theta/2}\right\},\quad t_c\ll t\ll\hat t_{p,b}\qquad(A.51)$$

Thus the factor Φ_p now becomes a very different factor, $\hat\Phi_p$, given by

$$\hat\Phi_p=\left(\hat k-k_p\right)\left[\left(\frac{\sigma}{\sigma_p}\right)^{\rho}\frac{t}{t_p}\right]^{\theta/2}\qquad(A.52)$$

Unfortunately θ is a very small number (e.g., $0.08<\theta<0.16$) for carbon fiber/epoxy composites. Thus the benefit of the proof test is very short-lived as $\hat\Phi_p$ rapidly approaches unity. Then the reliability rapidly becomes that of surviving the proof test itself.

We also notice that the difference between the stochastic fiber breakage model and the classic model tends to disappear for larger values of θ. In fact, for $\theta=2$ and noting $\beta\approx\alpha/\rho\approx\hat k\zeta/\left(2\zeta/\theta\right)\approx\hat k\theta/2=\hat k$ we see that $\Phi_p\approx\hat\Phi_p$ so the two results become the same. Typically θ growing larger corresponds to ρ becoming smaller, i.e. the composite is more susceptible to stress rupture overall. However the differences are most marked for the case of large ρ.

References

A.1   Phoenix, S. L., Schwartz, P. and Robinson IV, H. H., "Statistics for the Strength and Lifetime in Creep-Rupture of Model Carbon/Epoxy Composites," *Composites Science and Technology*, Vol. 32, 1988, pp. 81–120.

A.2   Otani, H., Phoenix, S. L., and Petrina, P., "Matrix Effects on Lifetime Statistics for Carbon Fiber/Epoxy Microcomposites in Creep-Rupture," *Journal of Materials Science*, Vol. 26, 1991, pp. 1955–1970.

A.3   Mahesh, S., and Phoenix, S. L., "Lifetime Distributions for Unidirectional Fibrous Composites under Creep-Rupture Loading", *Int. J. Fracture*, Vol. 127, 2004, 303–360.

A.4   Farquhar, D., Mutrelle, S. L., and Smith, R. L., "Lifetime Statistics for Single Graphite Fibers in Creep-Rupture," *Journal of Materials Science*, Vol. 24, 1989, pp. 2151–2164.

1. REPORT DATE (DD-MM-YYYY) 01-03-2010	2. REPORT TYPE Technical Memorandum	3. DATES COVERED (From - To)

4. TITLE AND SUBTITLE
Fiber Breakage Model for Carbon Composite Stress Rupture Phenomenon: Theoretical Development and Applications

5a. CONTRACT NUMBER

5b. GRANT NUMBER

5c. PROGRAM ELEMENT NUMBER

6. AUTHOR(S)
Murthy, Pappu, L.N.; Phoenix, S., Leigh; Grimes-Ledesma, Lorie

5d. PROJECT NUMBER

5e. TASK NUMBER

5f. WORK UNIT NUMBER
WBS 869021.03.03.02.01

7. PERFORMING ORGANIZATION NAME(S) AND ADDRESS(ES)
National Aeronautics and Space Administration
John H. Glenn Research Center at Lewis Field
Cleveland, Ohio 44135-3191

8. PERFORMING ORGANIZATION REPORT NUMBER
E-17092

9. SPONSORING/MONITORING AGENCY NAME(S) AND ADDRESS(ES)
National Aeronautics and Space Administration
Washington, DC 20546-0001

10. SPONSORING/MONITOR'S ACRONYM(S)
NASA

11. SPONSORING/MONITORING REPORT NUMBER
NASA/TM-2010-215831

12. DISTRIBUTION/AVAILABILITY STATEMENT
Unclassified-Unlimited
Subject Category: 24
Available electronically at http://gltrs.grc.nasa.gov
This publication is available from the NASA Center for AeroSpace Information, 443-757-5802

13. SUPPLEMENTARY NOTES

14. ABSTRACT
Stress rupture failure of Carbon Composite Overwrapped Pressure Vessels (COPVs) is of serious concern to Science Mission and Constellation programs since there are a number of COPVs on board space vehicles with stored gasses under high pressure for long durations of time. It has become customary to establish the reliability of these vessels using the so called classic models. The classical models are based on Weibull statistics fitted to observed stress rupture data. These stochastic models cannot account for any additional damage due to the complex pressure-time histories characteristic of COPVs being supplied for NASA missions. In particular, it is suspected that the effects of proof test could significantly reduce the stress rupture lifetime of COPVs. The focus of this paper is to present an analytical appraisal of a model that incorporates damage due to proof test. The model examined in the current paper is based on physical mechanisms such as micromechanics based load sharing concepts coupled with creep rupture and Weibull statistics. For example, the classic model cannot accommodate for damage due to proof testing which every flight vessel undergoes. The paper compares current model to the classic model with a number of examples. In addition, several applications of the model to current ISS and Constellation program issues are also examined.

15. SUBJECT TERMS
Composite overwrapped pressure vessels; Stress rupture; Weibull statistics; Stress rupture life; Liner loadsharing; Burst pressure; Operating pressure; Fiber strength; Pressurization rate; Power law; Confidence intervals; Reliability statistics

16. SECURITY CLASSIFICATION OF:			17. LIMITATION OF ABSTRACT	18. NUMBER OF PAGES	19a. NAME OF RESPONSIBLE PERSON STI Help Desk (email:help@sti.nasa.gov)
a. REPORT U	b. ABSTRACT U	c. THIS PAGE U	UU	30	19b. TELEPHONE NUMBER (include area code) 443-757-5802